Molecular Plant • Volume 1 • Number 5 • Pages 770–785 • September 2008 RESEARCH ARTICLE

A Novel C2-Domain Phospholipid-Binding Protein, OsPBP1, Is Required for Pollen Fertility in Rice

Wen-Qiang Yang[a,b], Ying Lai[a,b], Mei-Na Li[a,b], Wen-Ying Xu[a] and Yong-Biao Xue[a,1]

a Institute of Genetics and Developmental Biology, Chinese Academy of Sciences and National Centre for Plant Gene Research, Beijing 100190, China
b Graduate School of Chinese Academy of Sciences, Beijing 100049, China

ABSTRACT Pollen fertility is a crucial factor for successful pollination and essential for seed formation. Recent studies have suggested that a diverse range of internal and external factors, signaling components and their related pathways are likely involved in pollen fertility. Here, we report a single C2-domain containing protein, OsPBP1, initially identified through cDNA microarray analysis. *OsPBP1* is a single copy gene and preferentially expressed in pistil and pollen but down-regulated by pollination. OsPBP1 had a calcium concentration-dependent phospholipid-binding activity and was localized mainly in cytoplasm and nucleus, but translocated onto the plasma membrane in response to an intracellular Ca^{2+} increase. Pollen grains of antisense *OsPBP1* transgenic lines were largely nonviable, germinated poorly in vitro and of low fertility. OsPBP1 protein was localized in a region peripheral to pollen wall and vesicles of elongating pollen tube, and its repressed expression reduced substantially this association and led to alteration of microfilament polymerization during pollen germination. Taken together, these results indicate that OsPBP1 is a novel functional C2-domain phospholipids-binding protein that is required for pollen fertility likely by regulating Ca^{2+} and phospholipid signaling pathways.

Key words: rice (*Oryza sativa* L.); pollination; pollen fertility; OsPBP1; C2-domain; phospholipid.

INTRODUCTION

Pollination involves several important reproductive steps for seed and fruit formation in higher plants, including a series of notable events, such as pollen adhesion, hydration, germination, pollen tube growth, and guidance to the ovules (Johnson and Preuss, 2002). In rice, the process of pollination is well described. Firstly, pollen grains are released as a result of dehiscence of anthers stick to the brush-shaped stigma and start germinating after hydration. Secondly, the tip of pollen tube emerges from an aperture of a pollen grain, and the contents of the grain move into the pollen tube, including two sperm nuclei following a vegetative nucleus. Thirdly, the elongating tube begins to penetrate into the stigma through the transmitting tissues and eventually reaches the micropyle of ovule (Dai et al., 2006). In recent years, many signaling components, such as calcium, phospholipids, calmodulin, cyclic nucleoside, cytoskeletons, GTPases, and protein kinases and their related signaling pathways such as cytoskeletons organization, vesicles transport, protein kinases and phospholipid signaling and their cross-talks, have been identified to be important for pollination (Franklin-Tong, 2002; Honys and Twell, 2003; Dai et al., 2006; Malho et al., 2006; Moutinho et al., 2001; Yang and Poovaiah, 2003; Yokota et al., 2005; Malho et al., 2006).

As a crucial prerequisite for successful pollination, pollen fertility is influenced by a series of complex cellular interactions, biochemical changes, and signal transduction events and a number of internal and external factors. It is known that tapetum functions in anther development and pollen fertility by providing enzymes for callose dissolution and materials for pollen wall formation and development. Several factors have been identified to be essential for tapetum development. In *Arabidopsis*, *Tapetal Development and Function1* (*TDF1*) encodes a putative R2R3 MYB transcription factor and is highly expressed in the tapetum, meiocytes, and microspores during anther development, which plays a vital role in pollen fertility by regulating tapetum differentiation and function and callose dissolution (Zhu et al., 2008). *Arabidopsis Male Sterility1* (*MS1*) encodes a leucine zipper-like PHD-type transcriptional factor and its mutation affects pollen fertility by altering

[1] To whom correspondence should be addressed. E-mail ybxue@genetics.ac.cn, fax +86-10–6253 7814, tel. +86-10–6255 2880.

doi: 10.1093/mp/ssn035, Advance Access publication 21 July 2008
Received 29 April 2008; accepted 19 May 2008

formation of pollen exine and cytosolic components as well as tapetum development (Ito et al., 2007). Two *Arabidopsis* Glucan Synthase-Like (GSL1 and GSL5) callose synthases have been found to play essential but redundant roles in pollen development and fertility by affecting pollen germination and tube growth (Enns et al., 2005). In addition, pollen wall proteins were shown to be important for pollen fertility; for example, the Ruptured Pollen Grain1 (RPG1) was a plasma membrane protein required for pollen fertility by controlling exine pattern formation of microspores, primexine deposition, callose secretion, and pollen wall development in *Arabidopsis* (Guan et al., 2008). *Rice Immature Pollen1* (*RIP1*) is expressed at the late stage of pollen development, and the mutant of *rip1* showed delayed formation of starch granules and the intine layer and poor germination, indicating that *RIP1* is necessary for pollen fertility and germination (Han et al., 2006).

Surface molecules such as waxes initiate the signaling network necessary for pollen fertility. For example, the cuticular wax biosynthesis gene, *CUT1*, encodes a long chain fatty acid-condensing enzyme, which is required for cuticular wax biosynthesis and pollen fertility in *Arabidopsis* (Millar et al., 1999). The product of *Arabidopsis CER1* is involved in conversion of long-chain aldehydes to alkanes—a key step in wax biosynthesis (Aarts et al., 1995). *Wax Deficient Anther1* (*WAD1*) is involved in cuticle and wax production in rice anther walls and required for pollen development and fertility (Jung et al., 2006). In addition, oleosins (a group of lipid droplets) (Ruiter et al., 1997) and flavonoids (small aromatic molecules) (Hsieh and Huang, 2007) are also necessary for pollen fertility. For example, *Glycine Rich Protein17* (*GRP17*) promoted efficient synthesis of oleosins to ensure pollen fertility for pollination in *Arabidopsis* (Mayfield et al., 2001). Flavonols (a specific class of flavonoid, synthesized in the tapetum, later released into the locule, taken up and modified by the developing gametophyte) have a direct role in controlling pollen fertility (Mo et al., 1992; Ylstra et al., 1992). The disruption of chalcone synthase (CHS) (a key enzyme for flavonoids synthesis) reduced pollen fertility by affecting pollen germination and tube growth, and the kaempferol was sufficient to restore normal pollen germination and tube growth in vitro and full seed set in vivo, indicating the poor pollen fertility was due to failed pollen germination and tube growth (Mo et al., 1992).

Phospholipids have been shown to regulate pollen germination and tube growth directly through multiple signaling pathways involving changes in Ca^{2+} levels and endocytosis, exocytosis, and cytoskeleton rearrangement (Brill et al., 2000; Li et al., 2001; Yang and Poovaiah, 2003; Monteiro et al., 2005). For example, glycosylphosphatidylinositol (GPI) functions in anchoring proteins to cell surface in eukaryotes. *Arabidopsis* SETH1 and SETH2 proteins are involved in the first step of GPI biosynthesis and required for establishment and maintenance of pollen germination and polarized pollen tube growth (Lalanne et al., 2004). Nevertheless, the molecular regulation of pollen fertility is still poorly defined, especially in rice (*Oryza sativa* L.), an important staple crop for more than half of the world population.

A number of lipid-binding domains have been identified and characterized over the last few years (Meijer and Munnik, 2003). C2-domain is one of the important lipid-binding modules with affinity for Ca^{2+} and lipids and consists of approximately 130 residues in length, originally identified as the second of two conserved domains (Cl-C2) in the Ca^{2+}-dependent α, β, and γ isoforms of protein kinase C (Ono et al., 1989). As a group, C2-domains display a remarkable property of binding a variety of different ligands and substrates, including Ca^{2+}, phospholipids, phosphoinositides, and intracellular proteins (Cho and Stahelin, 2006). Previous crystal structural analyses showed that C2-domains have a common fold of conserved eight-stranded anti-parallel β-sandwich connected by surface loops to form two different topologies (Rizo and Sudhof, 1998). A large majority of C2-domains contain a cationic patch in the concave face of the β-sandwich, cationic β-groove, and vary in the size and the electrostatic among C2-domains, indicating an essential structural or functional role (Cho and Stahelin, 2006). Additionally, the Ca^{2+}-binding sites of Ca^{2+}-dependent C2-domains contain three Ca^{2+}-binding loops (CBL1, CBL2, and CBL3) located at one side of the domain, and two side chains, which are mostly aspartate (Bittova et al., 1999). Removal or mutation of one or more of the Ca^{2+}-coordinating side chains has been shown to convert Ca^{2+}-dependent C2-domains to Ca^{2+}-independent ones or vice versa (Bittova et al., 1999).

In animal and yeast, more than 150 C2-domain proteins have been identified as various signaling molecules, including protein kinases, lipid modification enzymes, pathogen resister, GTPase-activating proteins, ubiquitination enzymes, and neuron singaling molecules (Clark et al., 1991; Sossin et al., 1993; Maekawa et al., 1994; Perin et al., 1991; Dunn et al., 2004; Gallagher and Knoblich, 2006), and are involved in phospholipid binding, protein–protein interaction, signal transduction, membrane and vesicular trafficking, and cross-talk linkers (Maekawa et al., 1994; Geppert et al., 1994; Orita et al., 1995; Nalefski and Falke, 1996; Cho and Stahelin, 2006). Plant C2-domain proteins are classified into four groups (Kopka et al., 1998), and single C2-domain-containing proteins are only identified in plants. Limited data have suggested that plant C2-domain proteins appear to have diversified functions (Meijer and Munnik, 2003), including mRNA long-distance transport, plant growth and defense, membrane targeting and pollen tube growth (Xoconostle-Cazares et al., 1999; Jensen et al., 2000; Yang et al., 2006; Dowd et al., 2006; Hua et al., 2001; Asano et al., 2002; Kim et al., 2003). In this study, we report a novel functional single C2-domain protein, OsPBP1, from rice. Our results showed that it interacts with phospholipids in a calcium-dependent manner and is required for pollen fertility likely by mediating Ca^{2+} and phospholipid signaling pathways.

RESULTS

Identification of *OsPBP1* Gene from Rice

Our previous cDNA microarray analysis revealed a number of candidate cDNAs related to pollination and fertilization

(Lan et al., 2004). Among them, a cDNA encoding a putative phospholipid-binding protein containing a conserved N-terminal C2-domain was identified and designated as *OsPBP1* (*Oryza sativa Phospholipid Binding Protein1*). Further sequence analysis revealed that OsPBP1 protein comprises a single C2-domain and a short C-terminal extension. Homology search in GenBank (www.ncbi.nlm.nih.gov) revealed that it is a gene with five exons and four introns, and the exon lengths are 68, 63, 130, 115, and 59 base pairs, respectively (Supplemental Figure 1A). It has 435 base pairs in the predicted ORF encoding a polypeptide of 145 amino acids in length with a calculated molecular mass of 16 kDa (Supplemental Figure 1B). Database search showed that *OsPBP1* is localized on chromosome 4. Amino acid alignment showed a high degree of sequence homology of OsPBP1 to several C2-domain-containing proteins (Supplemental Figure 1C). Phylogenetic analysis showed that it belonged to a subfamily of single C2-domain proteins in plants (Supplemental Figure 2). These results showed that *OsPBP1* encodes a novel rice C2-domain protein.

Expression Analyses of *OsPBP1*

To examine the genomic organization of *OsPBP1*, DNA blot analysis showed that *OsPBP1* is a single copy gene in rice genome (Figure 1A), and Northern blot analysis showed that *OsPBP1* is expressed in pistil both before and after pollination (Supplemental Figure 3A). We also examined its expression using eight cDNA samples for real-time quantitative PCR analysis (Figure 1B). The results showed that the expression level of *OsPBP1* was the highest in pistil just before anthesis and pollination and decreased 5 h after pollination. Further analyses revealed that *OsPBP1* was expressed strongly in the pistil and down-regulated during pollination (Figure 1C), consistent with our previous finding (Lan et al., 2004). Affymetrix chip analyses showed that *OsPBP1* transcripts were expressed in all the reproductive tissues tested and also detected in root and leaf; in addition, the reproductive tissues and more *OsPBP1* transcripts were accumulated in the reproductive tissues than in the vegetative tissues (Figure 1D). To further confirm the expression profiles of *OsPBP1*, RT–PCR analysis was performed. In this assay, a strong expression of *OsPBP1* was

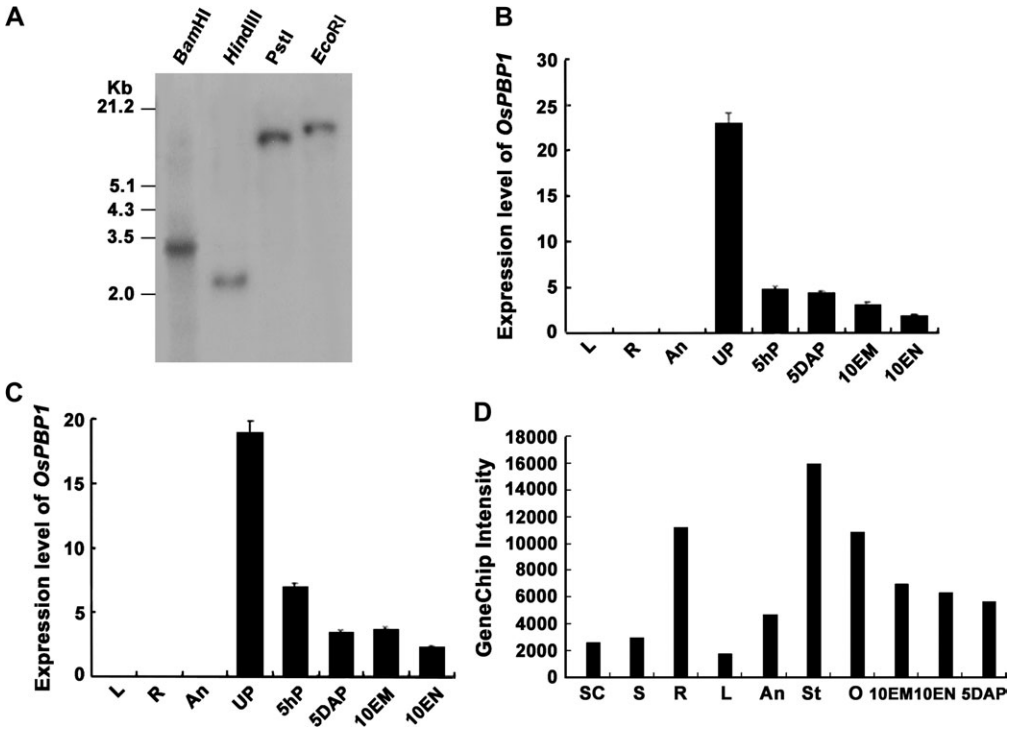

Figure 1. Genomic Organization and Expression Patterns of *OsPBP1*.

(A) Genomic DNA gel blot analysis of *OsPBP1* in rice. 5 mg of genomic DNA was restricted by *Bam*HI, *Pst*I, *Hin*dIII and *Eco*RI, respectively. The blot was hybridized with a probe specific for the *OsPBP1* coding region.

(B) Expression analysis of *OsPBP1* by qRT–PCR assay. L, leaf; R, root; An, anther; UP, unpollinated pistil; 5hP, pistil collected 5 h after pollination; 10EM, embryo collected 10 d after pollination; 10EN, endosperm collected 10 d after pollination. Error bars indicate standard errors of the mean ($n = 6$).

(C) Expression of *OsPBP1* based on cDNA microarray hybridization. The data were derived from a 10K rice cDNA microarray (Lan et al., 2004). Error bars indicate standard errors of the mean ($n = 3$).

(D) Affymetrix genechip analysis of *OsPBP1*. SC, suspension cell; S, seedling; St, stigma; O, ovary; 5DAP, embryo collected 5 d after pollination, and the other abbreviations are the same as that of (B).

detected in rice anther and pistil both before and after pollination and only weakly detected in root and seedling (Supplemental Figure 3B). Taken together, these results showed that *OsPBP1* is a single copy gene and mainly expressed in pistil and anther but down-regulated by pollination.

Sub-Cellular Localization of OsPBP1

To examine the sub-cellular localization of OsPBP1, we constructed a translational fusion between OsPBP1 and a synthetic green fluorescent protein (sGFP). The *OsPBP1-sGFP* fusion and s*GFP* alone, both driven by the cauliflower mosaic virus (CaMV) *35S* promoter, were introduced into onion epidermal cells by particle bombardment. The OsPBP1–GFP fusion protein was predominantly localized in the cytoplasm, in addition to the nucleus, while the control sGFP was uniformly distributed throughout the cell (Figure 2A and 2B). Similar results were also obtained in the transgenic *Arabidopsis* leaves (Supplemental Figure 4A). Furthermore, the sub-cellular localization of OsPBP1 protein in vivo was examined using a construct of *OsPBP1–sGFP* fusion driven by the *ubiquitin* promoter for transformation of *O. sativa* ssp. *Japonica* var. *Nipponbare*, and a total of nine transgenic T_0 lines were generated (data not shown). The results showed that the OsPBP1–GFP fusion protein was detected predominantly in the cytoplasm and nucleus in root cells of the transgenic plants (Figure 2C). These results suggest that the OsPBP1 protein localizes mainly in cytoplasm and nucleus.

OsPBP1 Binds Phospholipids In Vitro

Previous studies reported that most of the C2-domain proteins in mammalian and plants could interact with phospholipids in a calcium-dependent manner and involved in a phospholipid signaling pathway. To examine this possibility, the *OsPBP1* gene was expressed as a GST–OsPBP1 recombinant protein in *E. coli*, which was purified through an anion exchange chromatography (Figure 3A and 3B). The phospholipid-binding assay was carried out and the results showed that the GST–OsPBP1 protein had a weak binding activity with the ^{3}H-labeled PC/PS liposome in the absence of Ca^{2+}, and the negative controls, the glutathione-Sepharose 4B beads and GST protein

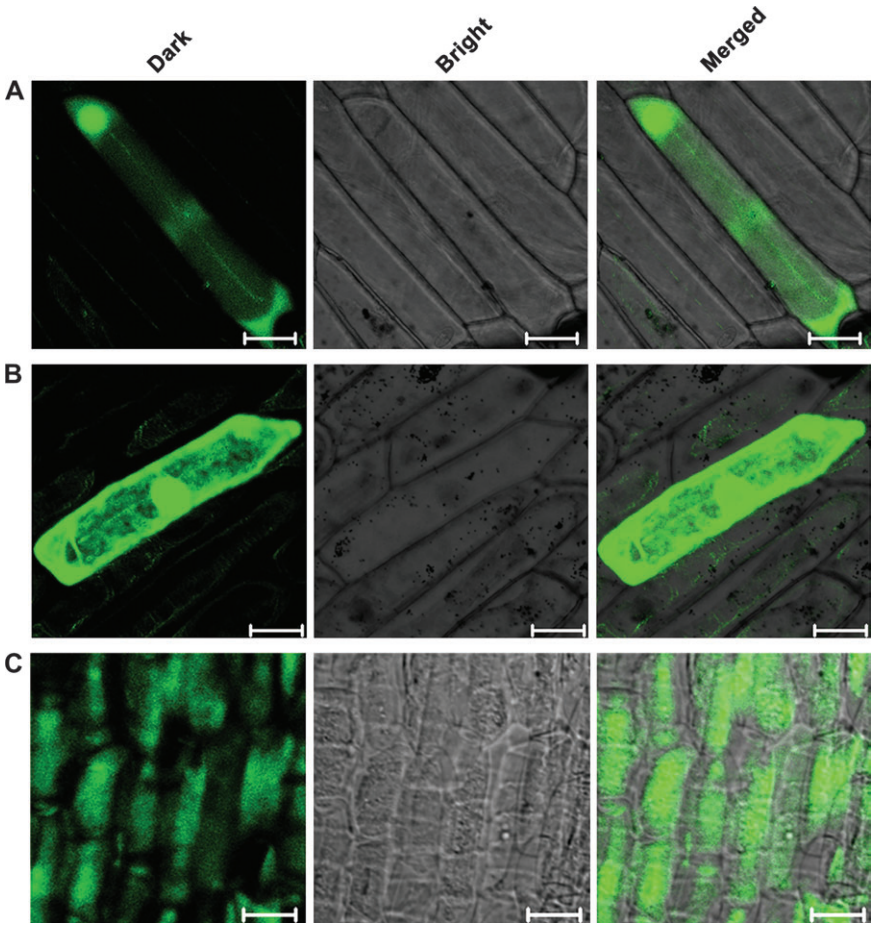

Figure 2. Sub-Cellular Localization of OsPBP1 Protein.

(A–B) Onion epidermal cells expressing the OsPBP1–green fluorescent protein (GFP) fusion protein and GFP alone driven by the *35S* promoter, respectively. Bars = 50 μm.

(C) Expression of the OsPBP1–GFP fusion protein driven by the *Ubiquitin* promoter in the root cells in the transgenic rice plant. Bars = 10 μm.

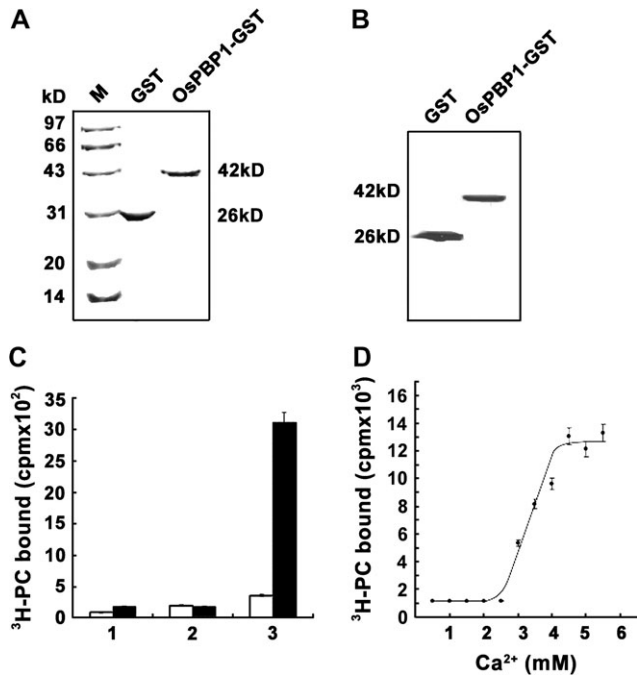

Figure 3. OsPBP1 Binds to Phospholipids in a Calcium-Dependent Manner.

(A) SDS–PAGE analysis of the purified GST (26 kD) and GST–OsPBP1 (42 kD) proteins with anion exchange chromatography. Lane M contained protein molecular weight markers as indicated.

(B) Western blot analysis of the purified GST and GST–OsPBP1 binding to glutathione sepharose-4B beads.

(C) Assay for Ca^{2+}-dependent phospholipid binding to the recombinant protein. Glutathione-sepharose beads, GST bound glutathione-sepharose beads or GST–OsPBP1 bound glutathione-sepharose beads (1, 2, and 3) were incubated with ^{3}H-labeled PC/PS liposome in the absence or presence of 1 mM Ca^{2+} (open or black column, respectively). Phospholipid binding was measured by liquid scintillation counting. Experiments were performed in triplicate with identical protein concentrations. Error bars indicate standard errors of the mean (n = 3).

(D) Analysis of Ca^{2+} concentration dependence of the phospholipid-binding activity of OsPBP1. The GST–OsPBP1 fusion protein bound to glutathione sepharose-4B beads was incubated with ^{3}H-labeled PC/PS liposome, with a series of free Ca^{2+} concentrations stabilized by Ca^{2+}/EGTA buffers. Error bars indicate the standard errors of the mean from three independent experiments.

had nearly no binding activity (Figure 3C). To verify the dependence of phospholipids-binding on the Ca^{2+} concentration, a series of $CaCl_2$ concentrations and a constant 2mM EGTA to chelated Ca^{2+} were used. The binding activity of GST–OsPBP1 protein to the PC/PS liposome was increased sharply to half-maximal under a final concentration of 1mM free Ca^{2+} and quickly reached a plateau at 2.5mM (Figure 3D). These results indicated that, in vitro, the OsPBP1 protein has a calcium concentration-dependent phospholipid-binding activity, suggesting that it is a functional phospholipid-binding protein and likely involved in a phospholipid signaling pathway.

Dislocation of OsPBP1 in Response to Intracellular Calcium Induction

To further examine the calcium-dependent phospholipid-binding activity of OsPBP1, we performed an intracellular calcium release experiment. A significant proportion of the OsPBP1–GFP fusion protein was translocated onto the plasma membrane following the treatment of the onion epidermal cells with Ca^{2+} solution containing the Ca^{2+}-mobilizing agonist ionomycin and its signal overlapped with the red fluorescence signal of FM 4–64, which produced yellow fluorescence on the plasma membrane (Figure 4A and 4B). Similar results were obtained in the transgenic *Arabidopsis* leaves, and the plasmolysis experiment showed that the fluorescence signal could be detected in the plasma membrane but not the cell wall (Supplemental Figure 4B and 4C). These results were further confirmed in root cells in the *OsPBP1–sGFP* transgenic plants in vivo (Figure 4C). Taken together, the results showed that OsPBP1 protein could be translocated onto the plasma membrane in response to intracellular Ca^{2+} increase.

Molecular and Phenotypic Analyses of the T_0 *OsPBP1* Antisense Transgenic Plants

To investigate the function of *OsPBP1* in vivo, a construct of *pCAMBIA1301-Ubi: OsPBP1-antisense* driven by the 35S promoter was transformed into *O. sativa* ssp. *Japonica* var. *Nipponbare* and *O. sativa* ssp. *Japonica* var. *Zhonghua 11* (Supplemental Figure 5A), and a total of nine independent T_0 lines were generated in two groups (A-1, A-2, and A-38 from *Zhonghua 11* and B-1 to B-6 from *Nipponbare*). Southern blot showed that all of them were positive transgenic rice plants, and Western blot analysis showed that the expression of OsPBP1 in all of them was reduced by various degrees (Supplemental Figure 5B and 5C).

Phenotypic analyses showed that no significant morphological differences were observed during vegetative development stages between the wild-type and the T_0 *OsPBP1* antisense transgenic lines, suggesting that its knockdown had no apparent effect on vegetative growth. However, the anthers in the transgenic line A-38 were shrunken, short, and bended (Supplemental Figure 6A), and, further, a poor seed set in the T_0 *OsPBP1* antisense transgenic lines were observed, indicating a reduction of OsBPP1 had affected the fertility (Supplemental Figure 6B). To examine this fertility alteration further, two test crosses were conducted. Crosses with the transgenic plant pollen on the wild-type showed poor seed set (38.9%), while crosses with wild-type pollen on the transgenic plants produced normal seed set (94%), suggesting an effect on the pollen fertility (Supplemental Figure 6C). To further examine the pollen fertility, the pollen dyeing with I_2-KI solution showed that less than 70% pollen grains could be stained in the *OsPBP1* antisense transgenic T_0 lines, while almost 100% of that in wild-type was stained. Among them, the pollen grains of A-38 were stained weakly and unevenly (Supplemental Figure 6D). To confirm the partial pollen fertility in the transgenic

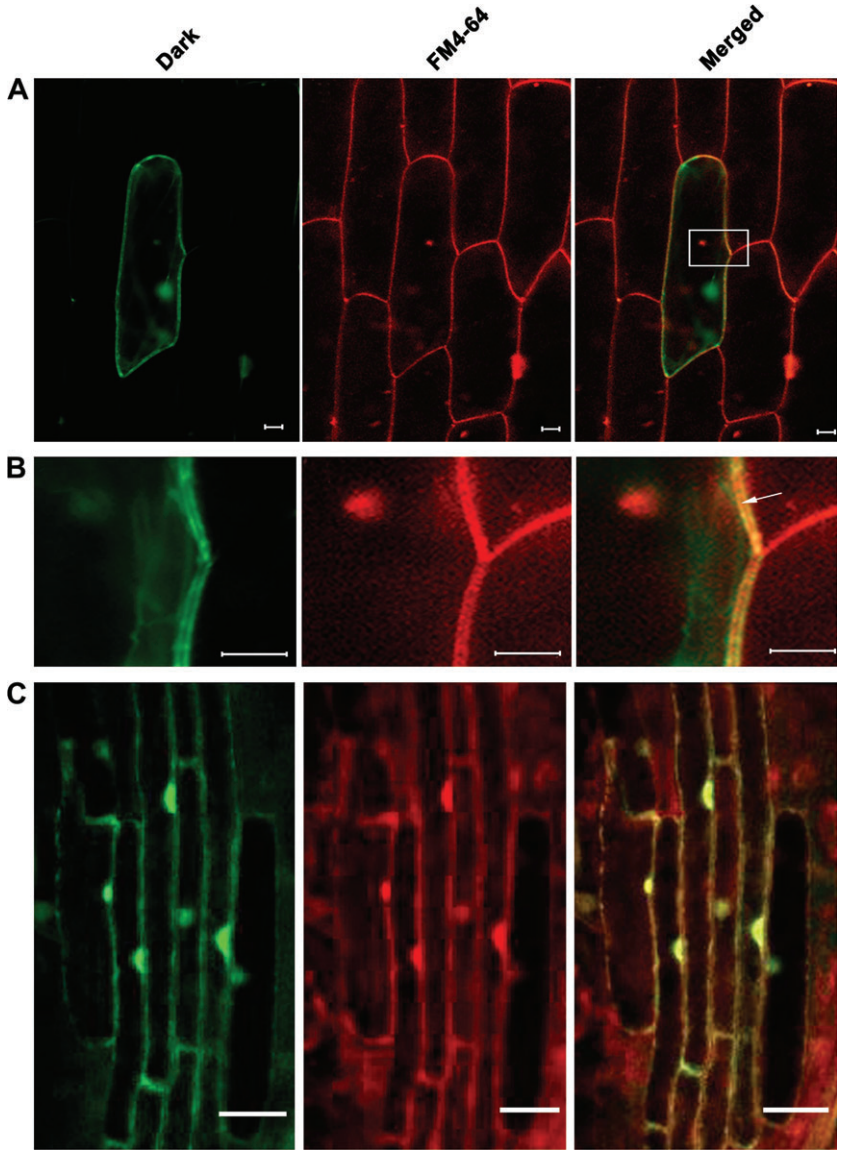

Figure 4. Accumulation of OsPBP1 in Cell Plasma Membrane after Intracellular Calcium Induction.

(A) The GFP–OsPBP1 fusion protein showed an accumulation in the plasma membrane after the onion epidermal cells were stimulated by Ca^{2+} solution containing the Ca^{2+}-mobilizing agonist ionomycin. The green fluorescence of OsPBP1–GFP fusion overlapped with the red fluorescence signal of FM 4-64, which formed yellow fluorescence. Bars = 15 μm.

(B) Enlarged pictures from (A). The arrows indicate the yellow fluorescence in the plasma membrane. Bars = 15 μm.

(C) Accumulation of the OsPBP1–GFP fusion in the plasma membrane when the root cells of the transgenic rice plant were stimulated by Ca^{2+} solution containing the Ca^{2+}-mobilizing agonist ionomycin. Bars = 20 μm.

plants, we stained the pollen by fluorescein diacetate (FDA) staining and found that the pollen viability in wild-type was better than that of the T_0 antisense transgenic line A-38 (Supplemental Figure 6E). Microscopy observation confirmed that the reduction of the *OsPBP1* transcripts affected the pollen development after the tetrad stage without affecting the pistil development (Supplemental Figures 7 and 8). These results suggested that the pollen grains in the *OsPBP1* antisense transgenic lines were largely nonviable and its expression reduction had an adverse effect on the pollen fertility.

Knockdown of *OsPBP1* Expression Led to Partial Pollen Fertility and Poor Seed Set

To further examine the phenotypes of the transgenic lines, 36 T_1 progeny of the *OsPBP1* antisense lines from eight independent T_0 lines and wild-type plants were grown in the field under similar conditions for the phenotypic analysis, and GUS staining assay and PCR were used to detect the positive antisense transgenic plants. The T_1 transgenic lines appeared normal during the vegetative growth, but the seed set of self-pollination of the T_1 progeny was drastically reduced in

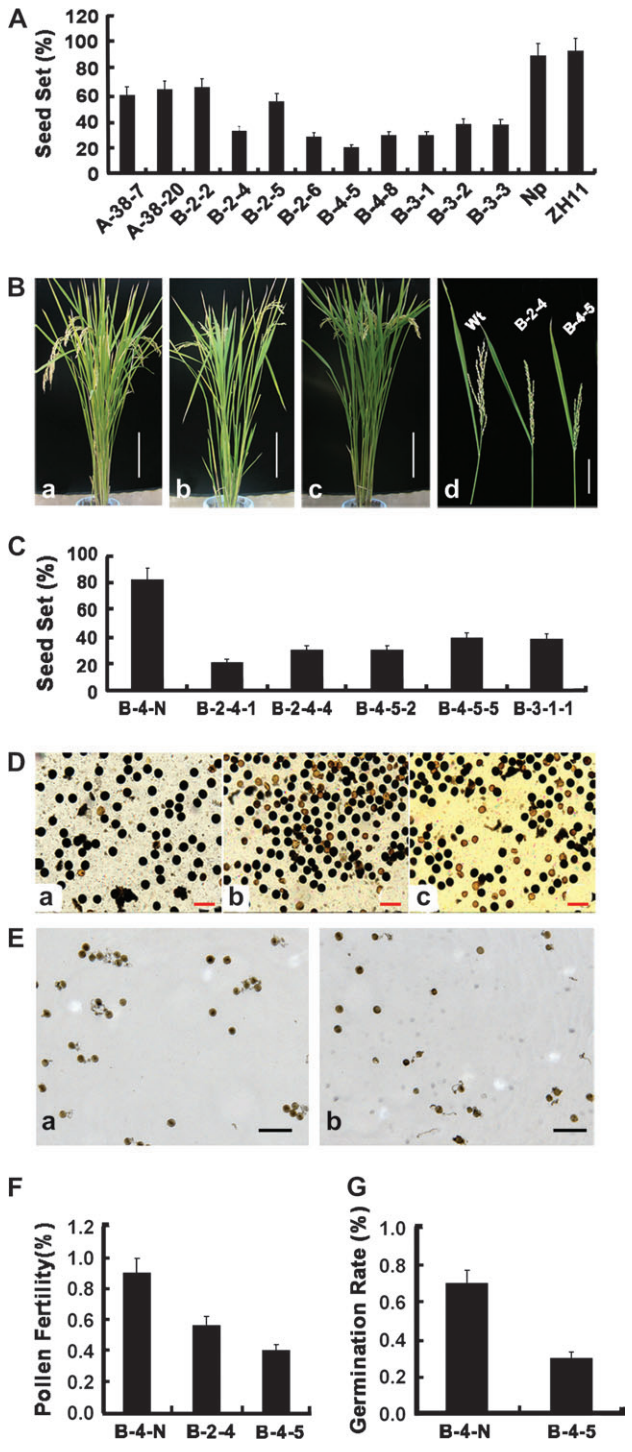

Figure 5. Phenotypic Analyses of Four Independent T_2 *OsPBP1* Antisense Transgenic Lines.

(A) Histogram of seed set of the T_1 positive *OsPBP1* antisense transgenic lines after self-pollination. A-38–7 and A-38–20 derived from A-38; B-2–2, B-2–4, B-2–5, and B-2–6 from B-2; B-4–5 and B-4–6 from B-4; and B-3–1, B-3–2, and B-3–3 from B-3. NP is the rice variety *Japonica* var. *Nipponbare* and ZH11 the *Japonica* var. *Zhonghua11*. Error bars indicate standard errors of the mean (n = 20).

(B) Gross morphology of the transgenic lines. B-4–N is a T_2 progeny without the transgene and used as a negative control (a). Two independent T_2 *OsPBP1* antisense transgenic lines B-2–4 (b) and B-4–5 (c) are shown at the ripening stage. Bars = 20 cm. The magnification of panicles of B-4–N, B-2–4, and B-4–5 showed decreased seed set after self-pollination (d). Bars = 15 cm.

(C) Histogram of seed set in the T_2 *OsPBP1* antisense lines. Error bars indicate standard errors of the mean (n = 20).

(D) Examination of pollen fertility of the transgenic T_2 lines. I_2-KI solution staining of the mature pollen grains from B-4–N (a) and the *OsPBP1* antisense transgenic plants, B-2–4 (b) and B-4–5 (c). The sterile pollen grains failed to be stained or stained weakly, indicating that they did not contain starch or contained irregularly distributed starch, whereas the viable pollen grains were stained deep brown. Bars = 50 μm.

(E) An in-vitro assay for pollen germination. The pollen grains from B-4–N (a) and *OsPBP1* antisense transgenic line B-4–5 (b) were collected just before anthesis and used for in-vitro pollen germination assay. Bars = 50 μm.

(F–G) Histogram of the frequencies of pollen staining by I_2-KI solution and pollen germination in vitro, respectively. Error bars indicate standard errors of the mean (n = 10).

the transgenic plants from three T_0 antisense transgenic lines: B-2, B-4, and B-3 (Figure 5A). Among them, the T_1 progeny of B-2 and B-4 with one single copy transgene were used for further analysis.

In total, five T_2 homozygous transgenic lines were obtained by using PCR and 50 mg ml^{-1} hygromycin screening (data not shown). Among them, two single copy insertion lines were derived from B-2 (B-2–4–1 and B-2–4–4), two from B-4 (B-4–5–2 and B-4–5–5) and one double copy insertion line from B-3 (B-3–1–3). Furthermore, Southern blot analysis with the *hygromycin* and *OsPBP1* probes of the T_2 *OsPBP1* antisense transgenic plants revealed that the *OsPBP1* antisense transgene were stably inherited (Supplemental Figure 9A). To examine the transcription levels of *OsPBP1* in the antisense transgenic T_2 plants, real-time quantitative PCR analysis was conducted using anther total RNA from five T_2 homozygous transgenic lines and one line of the T_2 progeny without the transgene (B-4–N) as a negative control. The results showed that its transcription in all of the five transgenic lines was reduced substantially. Among them, B-2–4–1 had a reduction of 60.9%, B-2–4–4 44.9%, B-4–5–2 64.7%, B-4–5–5 51.3% and B-3–1–3 51.7% (Supplemental Figure 9B). B-2–4–1 and B-2–4–4 were subsequently represented by B-2–4, B-4–5–2 and B-4–5–5 by B-4–5, respectively. These results demonstrated that stable *OsPBP1* antisense transgenic lines were generated with substantial reduction of the *OsPBP1* transcripts.

Phenotypic observation again showed that no significant morphological differences between the T_2 *OsPBP1* antisense homozygous transgenic lines (B-2–4 and B-4–5) and B-4–N during vegetative development stages (Figure 5B). The five T_2 homozygous transgenic lines showed a decreased seed set of various levels (Figure 5C), indicating that a repression of OsPBP1 had indeed affected the fertility. The results of test crosses supported the specific adverse effect of OsPBP1 on the pollen fertility (B-4–5 × wild-type, 81.3%, wild-type × B-4–5, 31.5%, and wild-type × wild-type, 80%; B-2–4 ×

wild-type, 85.1%, wild-type × B-2–4, 19.5%, and wild-type × wild-type, 80%). To further examine this role, we stained the pollen grains of the T_2 antisense transgenic lines B-2–4 and B-4–5 by using I_2-KI solution staining and found that they were irregularly shaped or pear-shaped and stained weakly and unevenly, containing a large central empty vacuole without any starch granule, typical for sterile pollen in rice, whereas almost all of the pollen grains of line B-4–N were round and dyed deep brown (Figure 5D and 5F). We also examined the pollen germination and found that the pollen grains of the B-4–N were germinated much better than that of B-4–5 (Figure 5E and 5G). These results confirmed that the reduced expression of OsBPB1 specifically affected the pollen fertility, suggesting a role of OsPBP1 in the pollen fertility control.

Detection of OsPBP1 Protein in Pollen and Pollen Tubes of the *OsPBP1* Antisense Transgenic Plants

To further examine the role of OsPBP1 in pollen, we determined the localization of OsPBP1 protein in pollen and pollen tube during pollen germination and pollen tube growth. The OsPBP1–yellow fluorescent protein (YFP) fusion protein was predominantly localized in a region peripheral to pollen wall and the yellow signal could be detected in the growing pollen tube (Supplemental Figure 10), indicating its membrane association. To confirm this finding in vivo, immunofluorescence blot assay was carried out by using the purified antibody of OsPBP1 and secondary antibody labeled by Alexa 488. Before pollination, the mature pollen grains of the B-4–5 and B-4–N were treated by a series of steps and observed by laser confocal microscope. In the B-4–N, the green fluorescence was detected in a region peripheral to pollen wall (Figure 6A). Furthermore, after pollen germination, the green fluorescence was detected mainly in vesicles of the elongating pollen tube (Figure 6B). However, the green fluorescence was only weakly detected in the pollen grains of the transgenic line B-4–5, whereas no green fluorescence could be detected in the rest pollen grains and tubes (Figure 6C and 6D). These results indicated that the OsPBP1 protein was associated with the pollen cell membrane and the vesicles of pollen tube and the repressed expression of *OsPBP1* reduced substantially this association, indicating a possible role of OsPBP1 in pollen germination.

Alterations of Microfilaments in Pollen and Pollen Tubes of the *OsPBP1* Antisense Transgenic Plants

To examine the role of OsPBP1 in pollen germination, we used phalloidin labeled by Alexa 488 to compare the pollen microfilament changes between the transgenic plants and wild-type. Before pollen germination, the microfilaments were arranged regularly towards the aperture in the B-4–N (Figure 7A), whereas they were diffused in the pollen grain of the B-4–5 (Figure 7B). After pollen germination, the polymerized microfilaments were detected in the pollen tube in the B-4–N (Figure 7C) but not in the B-4–5 (Figure 7D). To examine whether OsPBP1 could directly interact with actin, a co-localization experiment was performed by using the purified antibody of OsPBP1, the secondary antibody labeled by Alexa 488 and the Phalloidin labeled by Alexa 568 (Figure 7E). The results showed that the two fluorescence signals were not overlapped, suggesting that the OsPBP1 is not likely an actin binding protein (ABP). These results suggested that the *OsPBP1* reduction led to the alteration of the microfilament polymerization during pollen germination.

DISCUSSION

OsPBP1 Is a Novel Calcium-Dependent C2-Domain Phospholipid-Binding Protein

Our results showed that OsPBP1 encodes a single C2-domain protein capable of binding phospholipids in a calcium-dependent manner. But, it is unclear whether OsPBP1 is a general phospholipid or specific phospholipid-binding protein. The C2-domains could possess different lipid-binding capabilities as a function of Ca^{2+} concentration. In consistent, the quantity of phospholipids bound by OsPBP1 increased with Ca^{2+} concentration and obtained a high plateau of 2 mM Ca^{2+}. Lipid-binding specificity is determined by a specific lipid-binding site formed within a pocket, such as C1, PH, PX, and FYVE domains, or juxtaposed surface cationic residues, such as ANTH domain (DiNitto et al., 2003; Cho and Stahelin, 2006), while the proteins containing C2-domains do not have a well defined lipid-binding pocket or a conserved cationic patch for the specificity of lipid binding (Cho and Stahelin, 2006). The lipid specificity among the proteins containing C2-domain appears to be different; for example, OsERG1 could bind anionic phospholipids phosphatidylinositol (PI) and phosphatidylserine (PS), and very weak cationic phospholipids phosphatidylcholine (PC) and phosphatidylethanolamine (PE) (Kim et al., 2003). The specificity of PLCδ1 and PLCδ2 is anionic phospholipids and their preferential binding lipids are PS, PG, and PC (Ananthanarayanan et al., 2002). Furthermore, a majority of Ca^{2+}-dependent C2-domain-containing cationic residues in the Ca^{2+} binding loops prefer anionic lipids to zwitterionic ones and the cationic β-groove is now generally believed to bind anionic lipids. However, OsPBP1 contains five Ca^{2+}-binding Asp residues but binds both anionic PS and cationic PC, indicating that it is a novel type of C2-domain protein and binds phospholipids in a new manner.

The specificity of OsPBP1 for other phospholipids is unknown. Previous studies showed that the translocation of the C2-domain proteins is involved in Ca^{2+} signaling and membrane trafficking process, and the C2-domains of phospholipases, synaptotagmin I, ubiquitin protein ligase Nedd4, and protein kinase C have been shown to bind Ca^{2+} and they are transferred from the cytoplasm to the plasma membrane, thereby transducing a foreign signal into the cells (Rizo and Sudhof, 1998). Our results showed that OsPBP1 was localized in the cytoplasm and nucleus, but translocated onto the plasma membrane in a calcium-dependent manner, suggesting it is possibly involved in membrane trafficking and Ca^{2+} signaling pathway.

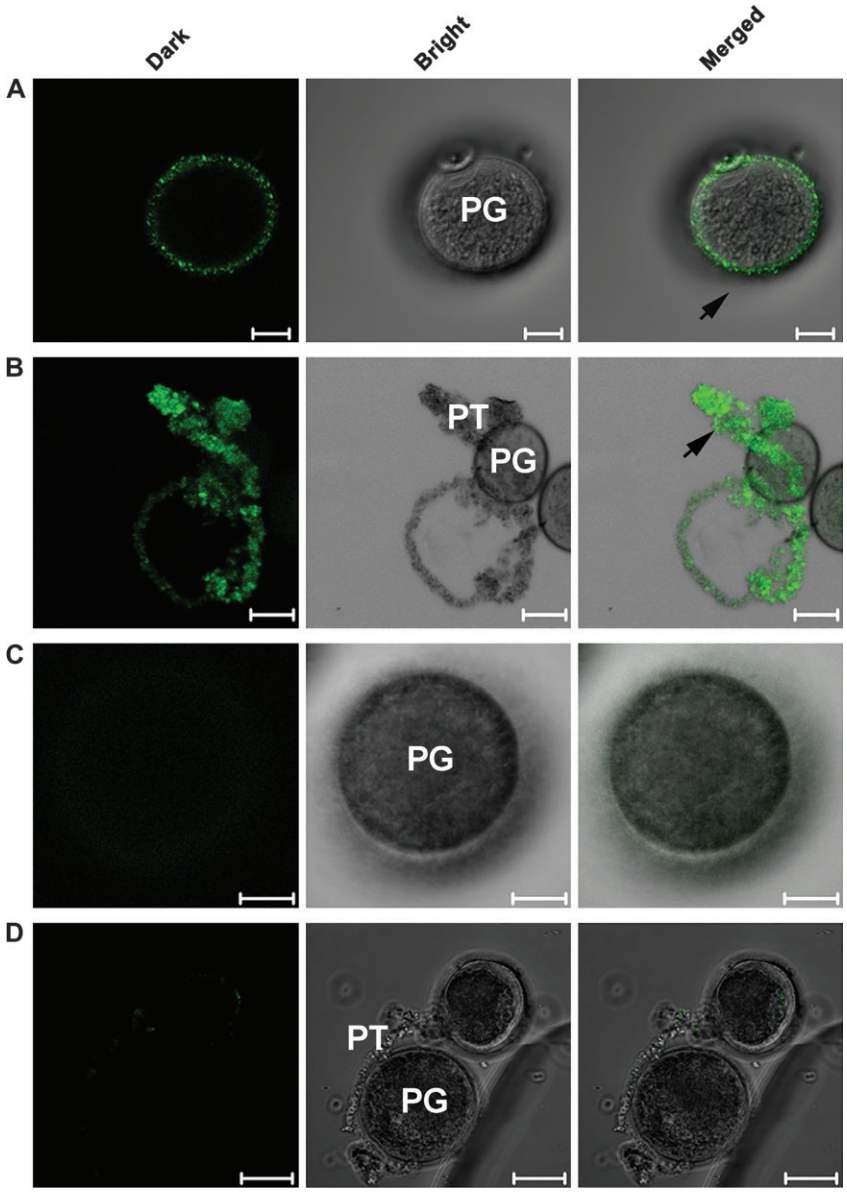

Figure 6. Immunolocalization of OsPBP1 in the Transgene-Negative Line B-4–N and the *OsPBP1* Antisense Transgenic Line B-4–5.

(A–B) Immunolocalization of OsPBP1 in pollen grains and pollen tube of the transgene-negative control line B-4–N, respectively. The arrows indicate the green fluorescence of OsPBP1 localized in a region peripheral to the pollen wall and in the pollen tube, respectively. Bars = 10 μm, 20 μm, respectively.

(C–D) Immunolocalization of OsPBP1 in pollen grains and pollen tube of the *OsPBP1* antisense transgenic T_2 line B-4–5, respectively. There is little green signal of OsPBP1 localizing in a region peripheral to the pollen wall and pollen tube, respectively. PG, pollen grain; PT, pollen tube. Bars = 10 μm, 20 μm, respectively.

However, it is unknown how OsPBP1 is targeted to the membrane. Three different roles have been proposed for Ca^{2+} in the membrane targeting of the C2-domain: acting as an electrostatic switch (Murray and Honig, 2002), inducing conformational changes in the calcium-binding regions (Bittova et al., 1999), and directly coordinating a lipid through calcium bridging or chelation (Verdaguer et al., 1999). Anionic lipid-selective C2-domains are I-type and PC-preferring C2-domains are H-type (Cho and Stahelin, 2006). For the I-type C2-domains, Ca^{2+} ions primarily function as an electrostatic switch or bridge and accelerates the association to the anionic membrane, while, in the case of the H-type cPLA2α C2-domains and the 5-lipoxygenase C2-domains, a Ca^{2+}-induced electrostatic neutralization in the Ca^{2+} binding loops has been proposed to promote the interfacial insertion of hydrophobic and aromatic residues (Cho and Stahelin, 2006). However, OsPBP1 binds both anionic and cationic possibly by utilizing both of the binding manners mediated by Ca^{2+} during its membrane translocation and targeting.

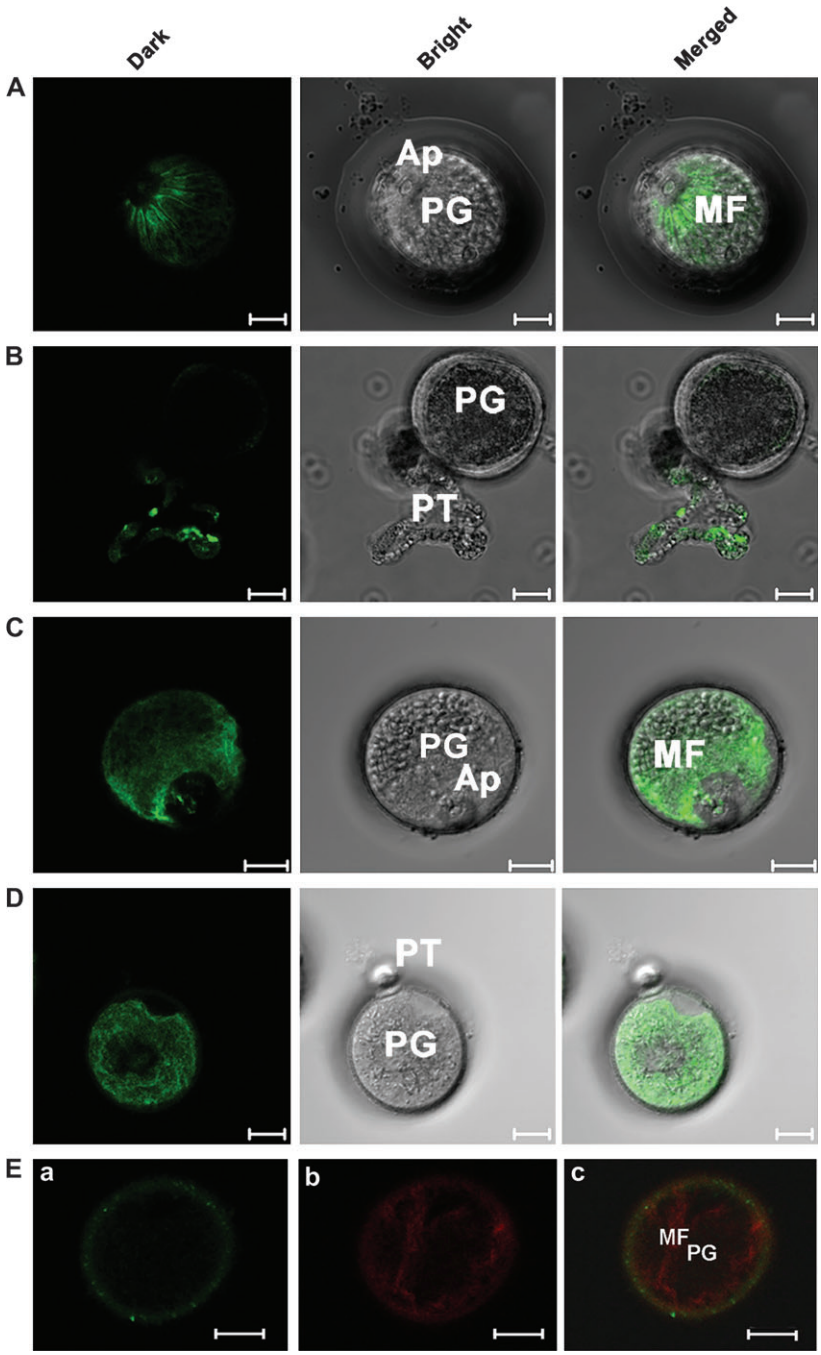

Figure 7. Dynamic Distribution of Microfilaments in the Transgene-Negative Line B-4–N and the *OsPBP1* Antisense Transgenic Line B-4–5.

(A–B) Dynamic distribution of microfilaments during pollen germination and in the pollen tube of the transgene-negative line B-4–N, respectively. The phalloidin labeled with Alexa 488 was used to detect the localizations of the polymerized microfilaments. The green signals represent the microfilaments in pollen grain and pollen tube. PG, pollen grain; PT, pollen tube; Ap, aperture; MF, microfilament. Bars = 10 μm, 20 μm, respectively.

(C–D) Dynamic distribution of microfilaments during pollen germination and in the pollen tube of the *OsPBP1* antisense transgenic T_2 line B-4–5, respectively. Bars = 10 μm.

(E) Co-localization of OsPBP1and microfilaments in pollen grain. The OsPBP1 was detected by its antibody staining (a) and the microfilaments by staining of phalloidin labeled with Alexa 568 (b). Their merged image is shown in (c). PG, pollen grain; MF, microfilaments. Bars = 10 μm.

Taken together, our findings show that OsPBP1 is a novel calcium-dependent C2-domain phospholipid-binding protein with a potential function as a molecular scaffold to facilitate signal transduction or vesicle trafficking.

OsPBP1 Is Required for Pollen Fertility and Germination

It has been shown that the C2-domain proteins are highly expressed in pollen, suggesting an important role in pollen development (Dai et al., 2006). A GTGA motif is localized in the promoter region of *G10*, a pollen-specific gene encoding pectin lyase to function in pollen (Rogers et al., 2001), and our results also showed that 10 GTGA motifs are localized in the promoter region of *OsPBP1*. Consistently, its knockdown substantially reduced the pollen fertility and germination rate.

However, it remains unclear how OsPBP1 affects the pollen fertility and germination. Phospholipid signaling regulates pollen germination possibly through altering the calcium concentration and signaling, GTPase activity and vesicle trafficking (Monteiro et al., 2005; Xue et al., 2007) or indirectly regulates pollen fertility similar to *Arabidopsis* SETH1 and SETH2 proteins (Lalanne et al., 2004). Our results showed that OsPBP1 could bind phospholipids; thus, it is possible that the low pollen fertility and the reduced pollen germination rate could result from a disassociation between OsPBP1 and phospholipids. However, the specific phospholipids bound to OsPBP1 are unclear, and the contribution of OsPBP1 as a signaling component in regulating pollen fertility and germination remains to be established.

It is unclear whether OsPBP1 is a cargo to be transported or to transport other cargoes. After binding the second messenger such as calcium, the conformation of some C2-domain proteins is changed to activate the phospholipid signaling pathway by interacting with downstream proteins, and a local Ca^{2+}-induced structural change has been observed or postulated for some C2-domains (Bittova et al., 1999). The C2-domains involved in protein–protein interactions such as DOC2γ C2A could bind nuclear import receptors and synaptotagmin I C2A binds syntaxin (Fukuda et al., 2001). Thus, it is possible that the C2-domain could be a linker between OsPBP1 and other proteins to function in controlling pollen fertility and germination. OsPBP1 is localized in the peripheral region of pollen wall and translocated onto the plasma membrane in a calcium-dependent manner, indicating that it likely acts by modulating calcium-dependent membrane trafficking or coupling calcium gradients and membrane trafficking during pollen germination. A large family of RAS-related small GTPases, Rabs or Ypts are known to regulate both anterograde and retrograde trafficking of transport vesicles between endomembrane compartments and the plasma membrane (Cheung et al., 2002). Profilin, a G-actin binding protein thought to be regulated by $PI(4,5)P_2$, is a potent controller of actin dynamics and found to be localized in the bulges of outgrowing pollen tubes (Lambrechts et al., 2002). Our results showed that the reduction of OsPBP1 appeared to lead to a diffused microfilaments distribution, suggesting that the transportation of necessary components along the cytoskeleton for pollen germination was disturbed, possibly through a disturbed regulation of phospholipids by OsPBP1.

In conclusion, our results show that OsPBP1 is a novel functional C2-domain phospholipid-binding protein and required for pollen fertility and germination. Further studies including using calcium inhibitors and identification of OsPBP1 targets will help to understand its detailed function in the signaling network controlling pollen fertility.

METHODS

Plant Materials and Growth Conditions

Rice (*Oryza sativa* sub. *Japonica* var. *Nipponbare* and var. *Zhonghua11*) was used in this study. Transgenic plants (antisense T_0, T_1, and T_2 lines) and untransformed negative control were grown in the field under natural conditions within two growing seasons, respectively. The growing season as well as their growth conditions were described previously (Kong et al., 2006).

Real-Time PCR

Total RNA from various tissues was isolated using the RNeasy Plant Minikit (Qiagen, Düsseldorf, GER), and real-time PCR were performed as previously described (Li et al., 2007). In brief, reverse transcription was performed using the TaqMan Reverse Transcription Regents kit (Applied Biosystems, Foster City, USA: ABI). The cDNA template samples were diluted to 5 and 1.25 ng μL^{-1}. Triplicate quantitative assays were performed on 2 μL of each cDNA dilution using the SYBR GreenMaster mix (ABI, PN 4309155) with an ABI 7900 sequence detection system according to the manufacturer's protocol (ABI). The gene-specific primers were designed by using PRIMEREXPRESS software (ABI). The relative quantification method (Delta–Delta CT) was used to evaluate quantitative variation between replicates examined. The amplification of 18S rRNA was used as an internal control to normalize all data. Gene-specific primers for *OsPBP1* were 5′-CGCACTGCATCGCTATGGT-3′ and 5′-GACTGCTCTTTTCAATAGGCTTTGT-3′, and for *18S rRNA* 5′-CGGCTACCAC ATCCAAGGAA-3′ and 5′-TGTCACTACCTCCCCGTGTCA-3′.

Northern Blot and RT–PCR Analyses

Total RNA from was prepared and digested with DNase I (TaKaRa, Dalian, China). Twenty-five microgram total RNA was electrophoresed on 1% denatured gel, and transferred onto Hybond N^+ membranes (Amersham, GeneQuant Pro, USA). Prehybridization, hybridization and washing of the blot were performed as recommended by the manufacturers. For RT–PCR, reverse transcriptase (Invitrogen, Carlsbad, USA) was used to synthesize the first strand cDNA. After 1:10 dilution, 2 μl of the synthesized cDNA was used for RT–PCR. PCR conditions were 30 cycles of 94°C for 1 min, 55°C for 1 min, 72°C for 1 min, and, finally, 72°C for 5 min. The specific primers of *OsPBP1* used for RT–PCR were 5′-ATGGTGCAG GGGACGCTC-3′

and 5′-TCAAGATGACTGCTTC-3′. The specific primers of tubulin used for RT–PCR were 5′-TTTGGAGCCTGGGACTATGGAT-3′ and 5′-AC GGGGGAATGGGATGAGAT-3′.

Southern Blot Analysis

Genomic DNA isolation and Southern blot analysis were performed as described previously (Lai et al., 2002). Five micrograms DNA was digested, separated on 0.8% agarose gel, and transferred onto Hybond Nt (Amersham, GeneQuant Pro, USA) membrane. Prehybridization, hybridization, and washing of the blot were performed as recommended by the manufacturers. *HPT* and *OsPBP1* probe was labeled with ^{32}P by random priming using the Prime-a-Gene labeling system (Promega, Madison, USA). The *HPT* primers were 5′-GCAAGGAATCGGTCAATACAC-3′ and 5′-TCCACT ATCGGCGAGTACTTC-3′, and the *OsPBP1* probe were 5′-ATGGTGCAGGGGAC GCTC-3′ and 5′-TCAAGATGACTGCTTC-3′.

Expression of OsPBP1 in *E. coli* and Antibody Preparation

A full-length *OsPBP1* cDNA was subcloned into *pGEM-4T3* bacterial expression vector between the *Eco*RI and *Sal*I sites in which the insert was fused to the C-terminal of GST, and the primers used were 5′-GAATTCGGTGCAGGGGACGTC-3′ and 5′-GTCGACTCAAGATGACTGCTTC-3′. The resulting construct was introduced into protease-deficient *E. coli* strain BL21. When OD_{600} of the bacterial culture reached 0.6, 0.25 mM IPTG was added to induce the recombinant protein produce for 15 h at 20°C. The collected bacterial cells were lysed by infiltration and the recombinant proteins were purified by ionic exchange column. Purified recombinant OsPBP1 was used to elicit polyclonal antisera production in rabbits. The OsPBP1 polyclonal antibody was purified using the Protein A resin column according to the manufacturer's instruction.

Western Blot Analysis

The purified proteins were incubated with glutathione (GSH)-Sepharose 4B beads (Amersham, GeneQuant Pro, USA) for 30 min at room temperature with gentle shaking, respectively. The beads were washed with solution A (50 mM HEPES, pH 7.4 and 0.1 M NaCl) and then centrifuged and boiled. Fifteen micrograms of GST and GST-OsPBP1 fusion proteins were incubated respectively with 10 μl of glutathione sepharose-4B beads at 28°C for 15 min with vigorous shaking. After centrifugation at 12 000 *g* for 2 min, the pellets were washed with the washing solution. The pellets were mixed with 20 μl SDS-PAGE sample solution and heated at 100°C for 5 min. The proteins were separated on 10% SDS-PAGE, and transferred onto PVDF (Amersham, GeneQuant Pro, USA) membrane. After blotting, the filters were blocked with 15% skimmed milk power in TBS-T (50 mM Tris, 150 mM NaCl, and 0.05% Tween 20, pH 7.5) for at least 8 h at room temperature. Then, the membranes were incubated with the anti-OsPBP1 polyclonal antibody (1:200) at 37°C for 1 h. The pre-immune serum served as a control. The secondary antibodies were alkaline phosphatase-conjugated goat anti-rabbit secondary antibody (Sigma, St Louis, USA) diluted 1:10 000 in TBS-T. Signals were detected with 0.33 mg mL^{-1} 4-NBT (nitroblue tetrazolium) and 0.165 mg mL^{-1} BCIP (5-bromo-4-chloro-3-indolyl phosphate) (Sigma, St Louis, USA) in alkaline phosphate buffer (100 mmol L^{-1} Tris, pH 9.5, 100 mmol L^{-1} NaCl, and 5 mmol L^{-1} $MgCl_2$).

Phospholipids and Calcium Binding Assays

Phospholipids were prepared by the Davletov and Südhof (1993) method. Twenty-five micrograms GST-OsPBP1 or GST proteins bound, respectively, to GSH-Sepharose 4B beads were re-suspended in 70 μl buffer A (containing either $CaCl_2$ or 2 mM EGTA), then mixed with 30 μl prepared ^3H-labeled liposome at room temperature for 15 min with vigorous shaking. After briefly being centrifuged, beads were washed three times with 1 ml buffer A (containing either $CaCl_2$ or 2 mM EGTA). Liposome binding was counted by liquid scintillation counter. Free Ca^{2+} concentrations in buffer A were calculated by the software of WEBMAX. From the software, the total Ca^{2+} concentration and corresponding free Ca^{2+} concentration (in parentheses) in buffer were followed: 1.0 mM (5.4e–5 mM), 1.5 mM (1.6e–4 mM), 2.0 mM (1e–2 mM), 2.5 mM (5e–1 mM), 3.0 mM (1.0 mM), 3.5 mM (1.5 mM), 4.0 mM (2 mM). All buffers were made from the Ca^{2+}-free water using a 0.1-M $CaCl_2$ standard solution.

Western Blot Analysis of Transgenic Plants

Preparation of plant total proteins from all of the tissues for expression profile analysis and anthers of transgenic and wild-type plants were performed as described previously (Qiao et al., 2004). Fresh materials were ground in liquid nitrogen and extracted in 50 mmol L^{-1} Tris buffer (pH 8.0) with 300 mmol L^{-1} NaCl, 10 mmol L^{-1} ethylenediaminetetraacetic acid (EDTA), 10 mmol L^{-1} DTT, and a protease inhibitor cocktail (Sigma, St Louis, USA) at a dilution of 1:100. The extraction mixtures were kept on ice for 15 min and then centrifuged for 10 min at 10 000 *g* to pellet cellular debris. Protein concentrations of the different fractions were estimated according to the method of Bradford. Then, the SDS-PAGE, prehybridization, hybridization, washing of the blot and detection were performed as described above.

Plasmid Constructs

OsPBP1

The resulting PCR product of *OsPBP1* CDS was digested with *Eco*RI and *Hin*dIII, and reversely inserted between the CaMV *35S* promoter and the nopaline synthase terminator of the vector pCambia 1301. The *OsPBP1* CDS was PCR amplified by Pyrobest DNA polymerase (TaKaRa, Dalian, CHN) using the wild-type genomic DNA as template. The construct was completely sequenced to ensure that it did not contain PCR or cloning errors. The PCR primers used were as follows: 5′-AAGAATCCTCAAGATGACTGCTTC-3′ (*Eco*RI site underlined) and 5′-GGAA GCTTATGGTGCAGGGGACGCTC-3′ (*Hin*dIII site underlined).

OsPBP1–GFP Fusion

The complete CDS of *OsPBP1* was amplified using two primers: 5′-CAGTCGAC ATGGTGCAGGGGACGCTC-3′ (*Sal*I site underlined) and 5′-CGGGATCCTCAA GATGACTGCTTCCA-3′ (*Bam*HI site underlined). The resulting PCR product was subcloned into a rebuilt vector *pCAMBIA1301* driven by maize *ubiquitin* promoter to generate *p1301–Ubi:OsPBP1–GFP* and a rebuilt vector *pBI221* driven by CaMV *35S* promoter to generate *p221–35S:OsPBP1–GFP*. The constructs were sequenced to verify the in-frame fusion and no nucleotide mutations.

OsPBP1–YFP Fusion

The complete CDS of *OsPBP1* was amplified using two primers: 5′-CGGGATCCA TGGTGCAGGGGACGCTC-3′ (*Bam*HI site underlined) and 5′-GGAAGCTTTCA AGATGACTGCTTCCA-3′ (*Hin*dIII site underlined). The resulting PCR product was subcloned into a rebuilt vector *pGreen II* driven by *LAT52* promoter to generate *pGreen–LAT52:OsPBP1–YFP* containing an *OsPBP1–GFP* fusion construct. The construct was sequenced to verify the in-frame fusion and no nucleotide mutations.

Plant Transformation and Generation of Transgenic Plants

Plant transformation was performed as previously described (Kong et al., 2006). Briefly, rice embryonic calli were induced on scutella from germinated seeds and transformed with strain EHA105 of *Agrobacterium tumefaciens* containing desired binary vector. Transgenic plants were selected in half-strength Murashige and Skoog medium containing 50 mg L^{-1} Hygromycin (Roche, Nutley, USA). Hygromycin-resistant plants from calli, defined as transgenic plants of T_0 generation, were transplanted into the field. T_0 plants were further used for Southern blot analysis. For phenotypic analysis of the *OsPBP1* antisense lines, seeds of both the *OsPBP1* antisense T_0 lines and the wild-type control were germinated and then transplanted into the field under identical conditions. The *OsPBP1* antisense T_1 and T_2 lines were identified and confirmed from T_0 progeny by β-glucuronidase staining and real-time PCR analysis. For analysis of localization of OsPBP1–GFP, hygromycin-resistant *p1301–ubi:OsPBP1–GFP* T_0 lines were confirmed by β-glucuronidase staining and were then used for observation.

Sub-Cellular Localization

The constructs of *p221–35S:OsPBP1–GFP* and *GFP* alone were transformed into onion epidermal cells and *Arabidopsis* leaves using gene gun (Bio-Rad, Hercules, USA). Transformed materials were incubated in dark at 28°C. FM 4–64 (50 μg ml^{-1}) was used as an indicator of plasma membrane. Expression and localization of OsPBP1–GFP fusion protein and GFP were observed with a Zeiss LSM 510 META confocal microscope (Zeiss, Jena, GER). The construct of *pGreen– LAT52:OsPBP1–YFP* was transformed into pollen grains using gene gun (Bio-Rad, Hercules, USA). The transformed onion epidermal cells were incubated in dark at 20°C to observe the localization of OsPBP1 in pollen grains and 28°C to observe the localization of OsPBP1 in pollen tube, respectively. Expression and localization of OsPBP1–YFP fusion protein was observed under a confocal laser scanning microscope (Zeiss, LSM 510). The *p1301–ubi:OsPBP1–GFP* construct was transformed into wild-type rice plants. The root tip of the transgenic rice plant was sectioned longitudinally and visualized with a laser-scanning confocal microscope (Zeiss, LSM 510).

Dislocation of OsPBP1 in Response to Intracellular Calcium Induction

Sub-cellular localization of OsPBP1 in onion epidermal cells, *Arabidopsis* leaves and root tip cells of transgenic rice were described as above. FM 4–64 (50 μg ml^{-1}) was used as an indicator of plasma membrane. The calcium agonist inomycin were used with 1 mM $CaCl_2$. Expression and localization of OsPBP1–GFP fusion protein and FM 4–64 were observed under a confocal laser scanning microscope (Zeiss, LSM 510).

Observations of Pollen Viability and Pollen Germination Assay

To evaluate pollen viability, mature anthers (before flowering) of *OsPBP1* antisense lines and wild-type plants were harvested and anthers before fertilization were dissected out from transgenic or wild-type plant. Pollen grains were released on a glass slide by gently squashing anther in a drop of staining solution. I_2-KI solution containing 1% (v/v) of I_2 in 3% (v/v) KI was used to check starch accumulation and fluorescein diacetate (FDA) was used to check pollen viability. Stained pollen grains were observed under an optical microscope. Mature anthers (before flowering) of *OsPBP1* antisense lines and wild-type plants were harvested by shaking panicles gently during flowering and transferred into a liquid germination medium (20% sucrose, 10% PEG4000, 3 mM $Ca(NO_3)_2 \cdot 4H_2O$, 40 mg L^{-1} H_3BO_3, 10 mg L^{-1} vitamin B1) and cultured for about 30 min at room temperature (~30°C) to germinate as in Dai et al. (2006). The pollen germination was observed under an optical microscope.

Cross-Pollination

Before flowering, rice flowers were emasculated and artificially pollinated for cross-pollination using pollen grains from transgenic plants and wild-type as pollen donor, respectively. After artificial pollination, the panicles were wrapped up to avoid cross-pollen. After maturation, the seed sets were observed.

Immunolocalization of OsPBP1 Protein in Pollen and Pollen Tube

Mature anthers of *OsPBP1* antisense lines and wild-type plants were harvested as above. To examine the localization of OsPBP1 in pollen grains, they were fixed in fixing solution (50 mM PIPES, 1 mM EDTA, 1 mM Mg^{2+}, 4% paraformaldehyde and 20% sugar) for 2 h, and the fixing solution was changed twice, then the samples were evacuated for 8 min. After incubation at room temperature for 45 min, the fixing solution was changed to 0.5 ml PBS buffer for 10 min three

times, the lytic solution (with 1% cellulase and pectinase) was added for 5 min, then triton-100 extraction for 10 min. After that, the samples were eluted by PBS buffer for 10 min three times, then added into 180 μl PBS buffer with 1% BSA and 0.05% NP40 and 20 μl purified antibody of OsPBP1 at 4°C overnight. Secondary antibody of Alexa-488-conjugated donkey anti-rabbit IgG (Eugene, OR, USA) was added into the solution at 1:1000 dilution at 37°C for 2 h in dark, and visualized localization of OsPBP1 with a Zeiss LSM 510 META confocal microscope using the following objective lens: 100-(Plan-APOCHROMAT, NA 1.4). The samples were excited at 488 nm with a krypton–argon laser, and the emission from the Alexa 488–fluorochrome was detected using a 505–530-nm bandpass filter. The antibody of OsPBP1 was purified by Protein A column. To examine the localization of OsPBP1 in pollen tube, pollen grains were treated to germinate as described by Dai et al. (2006).

Observation of Microfilaments Distribution in Pollen and Pollen Tubes

Mature anthers of *OsPBP1* antisense lines and wild-type plants were harvested as above. To observe microfilaments distribution in pollen grains, they were fixed in a fixing solution (with 50 mM PIPES, 1 mM EDTA, 1 mM Mg^{2+}, 4% paraformaldehyde and 20% sugar) for 2 h and the fixing solution was changed twice, then the samples were evacuated for 8 min. After 45 min at room temperature, the fixing solution was changed to 0.5 ml PBS buffer for 10 min three times, then a lytic solution (with 1% cellulase and pectinase) was added for 5 min. After Triton-100 extraction for 10 min, the materials were eluted by PBS buffer for 10 min three times, and added into 180 μl PBS buffer (with 50 mM PIPES, 1 mM EDTA, 1 mM Mg^{2+}, 0.05% NP40, 20% sugar and Phalloidin of Alexa-488 conjugated) for 10 min in dark and visualized the localization of microfilaments with a Zeiss LSM 510 META confocal microscope as described above.

Co-Localization of OsPBP1 Protein and Microfilaments Distribution

After treatment for immunolocalization, the recombinant OsPBP1 was added to a mixture of 190 ul PBS buffer (with 50 mM PIPES, 1 mM EDTA, 1 mM Mg^{2+}, 0.05% NP40, 20% sugar 4% and Phalloidin of Alexa-568 conjugated) for 10–20 min at room temperature and co-localization of OsPBP1 protein and microfilaments was visualized with a laser-scanning confocal microscope (Zeiss, LSM 510), as described above.

Histological Analysis

Plant materials fixed in FAA fixation solution were dehydrated through a graded ethanol series and embedded in Histonresin (Leica, Nussloch, Germany). Microtome sections (4 μm thick) were stained with 0.1% Toluidine-blue and visualized with an optical microscope.

Alignment and Phylogenetic Analysis

Sequence alignment of the C2-domain-containing proteins was performed using ClustalW. Phylogenetic analysis of the C2-domain-containing protein family based on amino acid sequences was carried out using a neighbor-joining (NJ) method with MEGA version 3.0. NJ analysis was done with the 'complete deletion' option selected. Support for each node was tested with bootstrap analysis, 1000 replicates for NJ, using a random input order for each replicate.

Accession Numbers

Sequence used in this study can be identified in NCBI GenBank data libraries under accession number CR282412.

SUPPLEMENTARY DATA

Supplementary Data are available at www.mplant.oxfordjournals.org.

FUNDING

This work was supported by the Ministry of Science and Technology of China (2005CB120804) and the Chinese Academy of Sciences.

ACKNOWLEDGMENTS

We thank Prof. Ming Yuan for providing assistance on localization of OsPBP1 and microfilaments. No conflict of interest declared.

REFERENCES

Aarts, M.G., Keijzer, C.J., Stiekema, W.J., and Pereira, A. (1995). Molecular characterization of the CER1 gene of arabidopsis involved in epicuticular wax biosynthesis and pollen fertility. Plant Cell. **7,** 2115–2127.

Ananthanarayanan, B., Das, S., Rhee, S.G., Murray, D., and Cho, W. (2002). Membrane targeting of C2 domains of phospholipase C-delta isoforms. J. Biol. Chem. **277,** 3568–3575.

Asano, T., Kusano, H., Okuda, T., Kubo, N., Shimada, H., and Kadowaki, K. (2002). Rpp16 and Rpp17, from a common origin, have different protein characteristics but both genes are predominantly expressed in rice phloem tissues. Plant Cell Physiol **43,** 668–674.

Bittova, L., Sumandea, M., and Cho, W. (1999). A structure–function study of the C2 domain of cytosolic phospholipase A2: identification of essential calcium ligands and hydrophobic membrane binding residues. J. Biol. Chem. **274,** 9665–9672.

Brill, J.A., Hime, G.R., Scharer-Schuksz, M., and Fuller, M.T. (2000). A phospholipid kinase regulates actin organization and intercellular bridge formation during germline cytokinesis. Development **127,** 3855–3864.

Cheung, A.Y., Chen, C.Y., Glaven, R.H., de Graaf, B.H., Vidali, L., Hepler, P.K., and Wu, H.M. (2002). Rab2 GTPase regulates vesicle trafficking between the endoplasmic reticulum and the Golgi bodies and is important to pollen tube growth. Plant Cell. **14,** 945–962.

Cho, W., and Stahelin, R.V. (2006). Membrane binding and subcellular targeting of C2 domains. Biochi. Biophy. Acta. **1761,** 838–849.

Clark, J.D., Lin, L.L., Kriz, R.W., Ramesha, C.S., Sultzman, L.A., Lin, A.Y., Milona, N., and Knopf, J.L. (1991). A novel arachidonic acid-selective cytosolic PLA2 contains a $Ca^{(2+)}$-dependent translocation domain with homology to PKC and GAP. Cell. **65,** 1043–1051.

Dai, S., Li, L., Chen, T., Chong, K., Xue, Y., and Wang, T. (2006). Proteomic analyses of *Oryza sativa* mature pollen reveal novel proteins associated with pollen germination and tube growth. Proteomics **6,** 2504–2529.

Davletov, B.A., and Sudhof, T.C. (1993). A single C2 domain from synaptotagmin I is sufficient for high affinity Ca^{2+}/phospholipid binding. J. Biol. Chem. **268,** 26386–26390.

DiNitto, J.P., Cronin, T.C., and Lambright, D.G. (2003). Membrane recognition and targeting by lipid-binding domains. Sci STKE **2003,** 16.

Dowd, P.E., Coursol, S., Skirpan, A.L., Kao, T.H., and Gilroy, S. (2006). Petunia phospholipase c1 is involved in pollen tube growth. Plant Cell. **18,** 1438–1453.

Dunn, R., Klos, D.A., Adler, A.S., and Hicke, L. (2004). The C2 domain of the Rsp5 ubiquitin ligase binds membrane phosphoinositides and directs ubiquitination of endosomal cargo. J. Cell Biol. **165,** 135–144.

Enns, L.C., Kanaoka, M.M., Torii, K.U., Comai, L., Okada, K., and Cleland, R.E. (2005). Two callose synthases, GSL1 and GSL5, play an essential and redundant role in plant and pollen development and in fertility. Plant Mol. Biol. **58,** 333–349.

Franklin-Tong, V.E. (2002). The difficult question of sex: the mating game. Cur. Opin. Plant Biol. **5,** 14–18.

Fukuda, M., Saegusa, C., Kanno, E., and Mikoshiba, K. (2001). The C2A domain of double C2 protein gamma contains a functional nuclear localization signal. J. Biol. Chem. **276,** 24441–24444.

Gallagher, C.M., and Knoblich, J.A. (2006). The conserved C2 domain protein lethal (2) giant discs regulates protein trafficking in Drosophila. Dev. Cell. **11,** 641–653.

Geppert, M., Bolshakov, V.Y., Siegelbaum, S.A., Takei, K., De Camilli, P., Hammer, R.E., and Sudhof, T.C. (1994). The role of Rab3A in neurotransmitter release. Nature **369,** 493–497.

Guan, Y.F., Huang, X.Y., Zhu, J., Gao, J.F., Zhang, H.X., and Yang, Z.N. (2008). RUPTURED POLLEN GRAIN 1 (RPG1), a member of MtN3/Saliva gene family, is crucial for exine pattern formation and cell integrity of microspores in *Arabidopsis thaliana*. Plant Physiol doi: 10.1104/pp.108.118026.

Han, M.J., Jung, K.H., Yi, G., Lee, D.Y., and An, G. (2006). Rice Immature Pollen 1 (RIP1) is a regulator of late pollen development. Plant Cell Physiol **47,** 1457–1472.

Honys, D., and Twell, D. (2003). Comparative analysis of the Arabidopsis pollen transcriptome. Plant Physiol **132,** 640–652.

Hsieh, K., and Huang, A.H. (2007). Tapetosomes in *Brassica tapetum* accumulate endoplasmic reticulum–derived flavonoids and alkanes for delivery to the pollen surface. Plant Cell. **19,** 582–596.

Hua, J., Grisafi, P., Cheng, S.H., and Fink, G.R. (2001). Plant growth homeostasis is controlled by the Arabidopsis BON1 and BAP1 genes. Genes Dev. **15,** 2263–2272.

Ito, T., Nagata, N., Yoshiba, Y., Ohme-Takagi, M., Ma, H., and Shinozaki, K. (2007). Arabidopsis MALE STERILITY1 encodes a PHD-type transcription factor and regulates pollen and tapetum development. Plant Cell. **19,** 3549–3562.

Jensen, R.B., Lykke-Andersen, K., Frandsen, G.I., Nielsen, H.B., Haseloff, J., Jespersen, H.M., Mundy, J., and Skriver, K. (2000). Promiscuous and specific phospholipid binding by domains in ZAC, a membrane-associated Arabidopsis protein with an ARF GAP zinc finger and a C2 domain. Plant Mol. Biol. **44,** 799–814.

Johnson, M.A., and Preuss, D. (2002). Plotting a course: multiple signals guide pollen tubes to their targets. Dev. Cell. **2,** 273–281.

Jung, K.H., et al. (2006). Wax-deficient anther1 is involved in cuticle and wax production in rice anther walls and is required for pollen development. Plant Cell. **18,** 3015–3032.

Kim, C.Y., et al. (2003). Rice C2-domain proteins are induced and translocated to the plasma membrane in response to a fungal elicitor. Biochemistry **42,** 11625–11633.

Kong, Z., Li, M., Yang, W., Xu, W., and Xue, Y. (2006). A novel nuclear-localized CCCH-type zinc finger protein, OsDOS, is involved in delaying leaf senescence in rice. Plant Physiol **141,** 1376–1388.

Kopka, J., Pical, C., Hetherington, A.M., and Muller-Rober, B. (1998). Ca2+/phospholipid-binding (C2) domain in multiple plant proteins: novel components of the calcium-sensing apparatus. Plant Mol. Biol. **36,** 627–637.

Lai, Z., Ma, W., Han, B., Liang, L., Zhang, Y., Hong, G., and Xue, Y. (2002). An F-box gene linked to the self-incompatibility (S) locus of Antirrhinum is expressed specifically in pollen and tapetum. Plant Mol. Biol. **50,** 29–42.

Lalanne, E., Honys, D., Johnson, A., Borner, G.H., Lilley, K.S., Dupree, P., Grossniklaus, U., and Twell, D. (2004). SETH1 and SETH2, two components of the glycosylphosphatidylinositol anchor biosynthetic pathway, are required for pollen germination and tube growth in Arabidopsis. Plant Cell. **16,** 229–240.

Lambrechts, A., Jonckheere, V., Dewitte, D., Vandekerckhove, J., and Ampe, C. (2002). Mutational analysis of human profilin I reveals a second PI(4,5)–P2 binding site neighbouring the poly(L-proline) binding site. BMC Biochem **3,** 12.

Lan, L., et al. (2004). Monitoring of gene expression profiles and isolation of candidate genes involved in pollination and fertilization in rice (*Oryza sativa* L.) with a 10K cDNA microarray. Plant Mol. Biol. **54,** 471–487.

Li, M., Xu, W., Yang, W., Kong, Z., and Xue, Y. (2007). Genome-wide gene expression profiling reveals conserved and novel molecular functions of the stigma in rice. Plant Physiol **144,** 1797–1812.

Li, Y., Zee, S.Y., Liu, Y.M., Huang, B.Q., and Yen, L.F. (2001). Circular F-actin bundles and a G-actin gradient in pollen and pollen tubes of *Lilium davidii*. Planta **213,** 722–730.

Maekawa, M., Li, S., Iwamatsu, A., Morishita, T., Yokota, K., Imai, Y., Kohsaka, S., Nakamura, S., and Hattori, S. (1994). A novel mammalian Ras GTPase-activating protein which has phospholipid-binding and Btk homology regions. Mol. Cel. Biol. **14,** 6879–6885.

Malho, R., Liu, Q., Monteiro, D., Rato, C., Camacho, L., and Dinis, A. (2006). Signalling pathways in pollen germination and tube growth. Protoplasma **228,** 21–30.

Mayfield, J.A., Fiebig, A., Johnstone, S.E., and Preuss, D. (2001). Gene families from the Arabidopsis thaliana pollen coat proteome. Science **292,** 2482–2485.

Meijer, H.J., and Munnik, T. (2003). Phospholipid-based signaling in plants. Annu. Rev. Plant Biol. **54,** 265–306.

Millar, A.A., Clemens, S., Zachgo, S., Giblin, E.M., Taylor, D.C., and Kunst, L. (1999). CUT1, an Arabidopsis gene required for cuticular wax biosynthesis and pollen fertility, encodes a very-long-chain fatty acid condensing enzyme. Plant Cell. **11,** 825–838.

Mo, Y., Nagel, C., and Taylor, L.P. (1992). Biochemical complementation of chalcone synthase mutants defines a role for flavonols in functional pollen. Proc. Natl Acad. Sci. U S A **89,** 7213–7217.

Monteiro, D., Castanho Coelho, P., Rodrigues, C., Camacho, L., Quader, H., and Malho, R. (2005). Modulation of endocytosis in pollen tube growth by phosphoinositides and phospholipids. Protoplasma **226,** 31–38.

Moutinho, A., Hussey, P.J., Trewavas, A.J., and Malho, R. (2001). cAMP acts as a second messenger in pollen tube growth and reorientation. Proc. Natl Acad. Sci. U S A **98,** 10481–10486.

Murray, D., and Honig, B. (2002). Electrostatic control of the membrane targeting of C2 domains. Mol. Cell. **9,** 145–154.

Nalefski, E.A., and Falke, J.J. (1996). The C2 domain calcium-binding motif: structural and functional diversity. Protein Sci. **5,** 2375–2390.

Ono, Y., Fujii, T., Igarashi, K., Kuno, T., Tanaka, C., Kikkawa, U., and Nishizuka, Y. (1989). Phorbol ester binding to protein kinase C requires a cysteine-rich zinc-finger-like sequence. Proc. Natl Acad. Sci. U S A **86,** 4868–4871.

Orita, S., Sasaki, T., Naito, A., Komuro, R., Ohtsuka, T., Maeda, M., Suzuki, H., Igarashi, H., and Takai, Y. (1995). Doc2: a novel brain protein having two repeated C2-like domains. Biochem. Biophy. Res. Com. **206,** 439–448.

Perin, M.S., Brose, N., Jahn, R., and Sudhof, T.C. (1991). Domain structure of synaptotagmin (p65). J. Biol. Chem. **266,** 623–629.

Qiao, H., Wang, F., Zhao, L., Zhou, J., Lai, Z., Zhang, Y., Robbins, T.P., and Xue, Y. (2004). The F-box protein AhSLF-S2 controls the pollen function of S-RNase-based self-incompatibility. Plant Cell. **16,** 2307–2322.

Rizo, J., and Sudhof, T.C. (1998). C2-domains, structure and function of a universal Ca2+-binding domain. J. Biol. Chem. **273,** 15879–15882.

Rogers, H.J., Bate, N., Combe, J., Sullivan, J., Sweetman, J., Swan, C., Lonsdale, D.M., and Twell, D. (2001). Functional analysis of cis-regulatory elements within the promoter of the tobacco late pollen gene g10. Plant Mol. Biol. **45,** 577–585.

Ruiter, R.K., Van Eldik, G.J., Van Herpen, R.M., Schrauwen, J.A., and Wullems, G.J. (1997). Characterization of oleosins in the pollen coat of *Brassica oleracea*. Plant Cell. **9,** 1621–1631.

Sossin, W.S., Diaz-Arrastia, R., and Schwartz, J.H. (1993). Characterization of two isoforms of protein kinase C in the nervous system of *Aplysia californica*. J. Biol. Chem. **268,** 5763–5768.

Verdaguer, N., Corbalan-Garcia, S., Ochoa, W.F., Fita, I., and Gomez-Fernandez, J.C. (1999). $Ca^{(2+)}$ bridges the C2 membrane-binding domain of protein kinase Calpha directly to phosphatidylserine. EMBO J **18,** 6329–6338.

Xoconostle-Cazares, B., Xiang, Y., Ruiz-Medrano, R., Wang, H.L., Monzer, J., Yoo, B.C., McFarland, K.C., Franceschi, V.R., and Lucas, W.J. (1999). Plant paralog to viral movement protein that potentiates transport of mRNA into the phloem. Science **283,** 94–98.

Xue, H., Chen, X., and Li, G. (2007). Involvement of phospholipid signaling in plant growth and hormone effects. Cur. Opin. Plant Biol. **10,** 483–489.

Yang, H., Li, Y., and Hua, J. (2006). The C2 domain protein BAP1 negatively regulates defense responses in Arabidopsis. Plant J **48,** 238–248.

Yang, T., and Poovaiah, B.W. (2003). Calcium/calmodulin-mediated signal network in plants. Trends Plant Sci. **8,** 505–512.

Ylstra, B., Touraev, A., Moreno, R.M., Stoger, E., van Tunen, A.J., Vicente, O., Mol, J.N., and Heberle-Bors, E. (1992). Flavonols stimulate development, germination, and tube growth of tobacco pollen. Plant Physiol **100,** 902–907.

Yokota, E., Tominaga, M., Mabuchi, I., Tsuji, Y., Staiger, C.J., Oiwa, K., and Shimmen, T. (2005). Plant villin, lily P-135-ABP, possesses G-actin binding activity and accelerates the polymerization and depolymerization of actin in a Ca^{2+}-sensitive manner. Plant Cell Physiol **46,** 1690–1703.

Zhu, J., Chen, H., Li, H., Gao, J.F., Jiang, H., Wang, C., Guan, Y.F., and Yang, Z.N. (2008). Defective in tapetal development and function1 (TDF1) is essential for anther development and tapetal function for microspore maturation in Arabidopsis. Plant J doi: 10.1111/j.1365–313X.2008.03500.x.